RESULTS FROM THE LCLS X-BAND TRANSVERSE DEFLECTOR WITH FEMTOSECOND TEMPORAL RESOLUTION

Y. Ding, F.-J. Decker, V. A. Dolgashev, J. Frisch, Z. Huang, P. Krejcik, H. Loos, A. Lutman, A. Marinelli, T. J. Maxwell, D. Ratner, J. Turner, J. Wang, M.-H. Wang, J. Welch, and J. Wu
SLAC National Accelerator Laboratory, Menlo Park, CA 94025, USA
C. Behrens
DESY, 22607 Hamburg, Germany

Abstract

An X-band RF transverse deflector composed of two 1-m-long X-band deflecting structures has been recently commissioned at the Linac Coherent Light Source (LCLS) at SLAC National Accelerator Laboratory. Located downstream of the FEL undulator, this device provides electron beam longitudinal phase space diagnostics in both time and energy which enables reconstruction of the X-ray FEL power profiles with an unprecedented resolution. This talk reports on the progress of this new LCLS X-band transverse deflector, first usage experience and measured results.

INTRODUCTION

Over the past several years, great progress has been made in the realization of high power X-ray free-electron lasers (FELs) [1–4]. The typical pulse duration from these sources can vary from several hundred femtoseconds down to a few femtoseconds, which enables ultrafast time-resolved X-ray studies with atomic spatial resolution. However, tremendous challenges remain in diagnosing such X-ray pulses with femtosecond temporal resolution. The measurement of X-ray pulses on the femtosecond time scale is a hot topic in the past years and several techniques have been recently studied (see a review paper [5]).

We previously proposed characterizing the X-ray temporal structure by measuring the lasing footprint left on the "parent" of the X-ray pulse: the electron beam [6]. An X-band radio-frequency (rf) transverse cavity (XTCAV) is adopted in conjunction with an electron beam energy spectrometer to measure the electron beam longitudinal phase space (time-energy) downstream of the FEL undulator. Since the lasing process in an FEL induces both electron energy loss and energy spread growth, the output electron longitudinal phase space can indicate the X-ray pulse information. Recently demonstrated at LCLS [7], this approach is simple and robust. It provides a single-shot measurement and is non-invasive to the FEL operation. The achieved temporal resolution is ~1 fs rms at soft X-ray energy and ~4 fs rms at hard X-ray energy. We discuss the XTCAV status and summarize recent experimental results at LCLS in this paper.

DIAGNOSTIC METHOD AND LAYOUT

In the FEL process, the interaction between an electron beam and an electromagnetic wave causes electron energy loss and energy spread increase. For example, at LCLS, the typical FEL-induced electron energy loss at saturation is more than 10 MeV [2]. By measuring the electron longitudinal phase space in FEL-on and FEL-off conditions, we can retrieve the time-resolved electron beam energy loss or energy spread increase due to the FEL lasing process. In this way the x-ray temporal profile can be obtained if the FEL slippage effect is small. The key point is to design a transverse deflector with high temporal resolution. In the deflecting mode, the time variation of the transverse fields is used to create a temporal-spatial correlation in the electron bunch phase space. The resulting image on a downstream screen forms a "streak" of the electron bunch, from which the pulse duration and temporal profile can be obtained [8,9]. The resolution is determined by the deflector frequency and voltage, together with beam properties (detailed discussion can be found in the supplementary materials of ref. [7]). By choosing an X-band frequency (11.424 GHz), it produces a faster, stronger transverse sweep of the beam, improving the temporal resolution over previous deflector designs such as S-band deflectors.

The sketch in Fig. 1 shows the implementation of the deflecting system at the LCLS. Two 1-m long X-band rf deflecting structures provide a 45 MeV/c nominal time-dependent horizontal kick to the beam [10]. The pre-existing, vertical-bend dipole magnet is used to measure the electron energy spectrum. A camera monitors the downstream cerium-doped yttrium aluminum garnet (Ce:YAG) crystal screen, capturing the transverse beam image. In this arrangement, the horizontal dimension of the measured image represents time while the vertical dimension represents energy.

Once the electron longitudinal phase space is measured, we can retrieve the X-ray temporal profile by comparing the lasing-off and lasing-on electron phase space. The electron current profile, time-sliced mean energy, and sliced energy spread are then computed to calculate the photon power profile. As mentioned earlier, the FEL lasing induces both electron energy loss and energy spread growth. By conservation of energy, we can first relate changes in the mean slice energy to instantaneous FEL power. Namely, the energy loss by each time slice of the electron bunch is given to the instantaneous power of the co-propagating FEL pulse as

$$P(t) = [\langle E\rangle_{FELoff}(t) - \langle E\rangle_{FELon}(t)] \times I(t)/e. \quad (1)$$

This work was supported at SLAC by the US Department of Energy under contract DE-AC02-76SF00515 and BES.

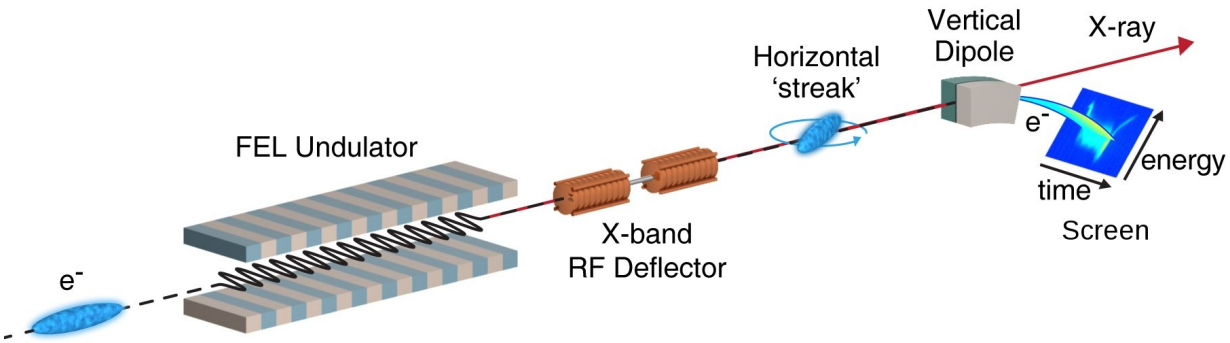

Figure 1: Diagnostic layout of the X-ray temporal measurement. It includes the transverse deflector, the magnetic spectrometer and the Ce:YAG screen located downstream of the FEL undulator. Two 1-m long X-band rf deflecting structures provide horizontal streaking followed by a vertical-bend dipole magnet for measuring the energy spectrum. A camera captures the transverse images of the electron beam density distribution on the diagnostic screen. The plot is from [7].

Where $P(t)$ is the FEL power, $E(t)$ is the time-sliced mean beam energy (for FEL on and off case), and $I(t)$ is the beam current. Note with the measured sliced energy loss and current, the absolute X-ray power can be directly obtained from Eq. (1).

A second relationship between the instantaneous FEL power and energy spread growth can also be derived. In the exponential gain regime (before saturation), the FEL power can be written approximately as [11]

$$P(t) \propto [\sigma^2_{E,FELon}(t) - \sigma^2_{E,FELoff}(t)] \times I^{2/3}(t) \quad (2)$$

where $\sigma_E(t)$ is the RMS slice energy spread and the constant of proportionality is unknown related to parameters not included in this measurement, such as the beam emittance. The 2/3 power scaling of beam current follows from an additional factor of the FEL efficiency parameter ρ which is proportional to $I^{1/3}$. In this energy spread method, we use the measured X-ray pulse energy from the gas detector to obtain the absolute X-ray power by normalization. In fact, due to the energy jitter in a real machine, for the energy loss method from Eq. (1), we typically also use the gas detector readings to offset the energy jitter effect.

XTCAV EXPERIMENTAL RESULTS

XTCAV Status

The idea of adding an X-band deflector at LCLS was initiated around 2006 [12], and its structures and power couplers were developed in the years that followed [15–17]. With the new potential to reconstruct the X-ray temporal shape [6], the XTCAV project at LCLS was officially supported to start in 2011. Since then, rapid progress has been made for the different parts of the system, including the structure fabrication and tuning, klystron and modulator, waveguides, controls, and so on [10, 14]. By the end of May 2013, the full system was online and ready for commissioning. Commissioning went very smoothly, and the device started to serve some user experiments in the fall of 2013 with the data recorded in the accelerator main control room. Since the spring of 2014, the data acquisition was upgraded so the users can record the XTCAV images together with their experimental data in the experimental hutch at 120 Hz full beam rate. The single-shot X-ray pulse temporal diagnostic at full LCLS beam rate has been established.

X-ray Pulse Profile Reconstruction

The direct application of the XTCAV is to measure the electron bunch and X-ray pulse durations and shapes. We reported this study in other publications [7, 11, 13]. Here we take one example from [7] to illustrate this technique.

As shown in Fig. 2, the electron beam energy is 4.7 GeV with FEL operating at a resonant photon energy of 1.0 keV. We first suppressed the lasing process by perturbing the electron horizontal trajectory at the beginning of the undulator and then recorded hundreds of what we refer to as "lasing-off" or "baseline" longitudinal phase space images on the screen. Figure 2 panel (a) shows a typical single-shot baseline image. Its projection onto time gives the electron bunch current profile. Next we restored the electron trajectory and recorded the "lasing-on" images for normal operation case (a single-shot is shown in panel (b)). Comparing panel (b) with (a), one can clearly see the time-resolved energy loss and energy spread growth due to the lasing process. By applying the two equations discussed earlier, the X-ray temporal profile can be retrieved as shown in panel (c).

Lasing Evolution of Soft X-ray FELs

With the capability to measure the electron beam longitudinal phase space and to reconstruct X-ray temporal profile, we can study the FEL lasing evolution along the undulator position. To do this, we just suppress the lasing over a section of the undulator by perturbing the electron trajectory

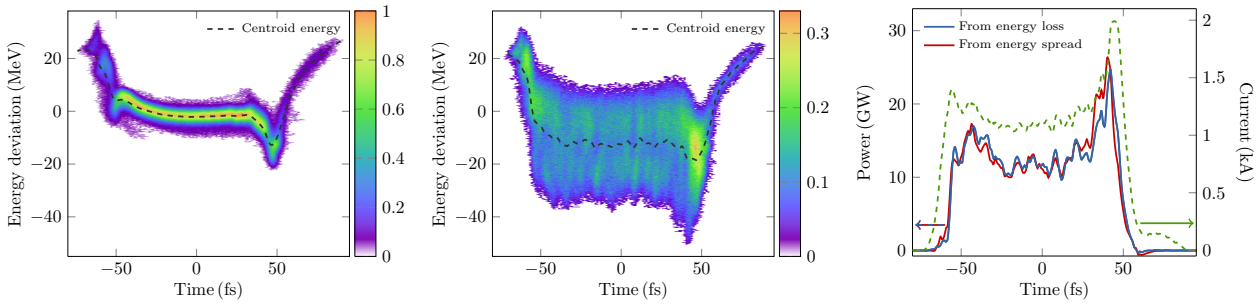

(a) Lasing off (b) Lasing on (c) Temporal profiles

Figure 2: Temporal profile reconstruction. The electron bunch charge is 150 pC with an energy of 4.7 GeV to produce photons at 1.0 keV. The measured single-shot longitudinal phase space images are shown in (a): “lasing off" and (b): “lasing on". The reconstructed X-ray power profiles are shown in (c) from the time-dependent energy loss (blue curve) and energy spread growth (red curve). The bunch head is to the left in these plots and throughout. The plots are from [7].

with corrector magnets located along the undulator. Here we show one example for soft X-ray energy at 1keV with 150pC. The measured power gain curve starts to roll over around undulator 12 (U12). In the figure 3, we show one lasing-off image, and the lasing-on images at U9, U15, U21, U27 and U33, with the reconstructed X-ray profiles as well. We can see clearly the energy spread increases along the undulator. After U20, there is a hint that some particles are trapped in the lasing process since there seems a vague energy gap on the time-energy images. However, at the end of the undulator (U33), the trapping feature is washed out as although more photons are obtained from the higher energy electrons. This could be due to the limited taper range for soft X-ray FELs with the existing LCLS undulators.

Particle Trapping After Saturation

We observed much clearer particle trapping at hard X-ray energies. The trapping has been discussed in many other books and papers (see, e.g., [18]). The post-saturation taper [19] plays an important role here. After saturation, due to a relatively large energy loss on the electrons, the undulator strength (K value) has to be tapered along the z direction to match the electron energy loss so that the FEL resontant condition is still satisfied. In this tapering configuration, some electrons are able to be continuously trapped within the longitudinal phase space separatrix (or “radiation bucket") for lasing.

Two example images are shown here with photon energy 7.7 keV and 6.0 keV in Fig. 4. In the energy dimension, clear separate energy bands are observed. In the 7.7 keV case, we see two additional stripes at the low energy side. And in the 6.0 keV case, we even see about 5 energy stripes. As discussed earlier, after FEL saturation, some electrons are being kept in the radiation bucket. But with long enough tapered undulator, a fraction of the trapped particles might get lost due to continuously increased energy spread. In this way, those particles out of the bucket will stay at a constant energy level (the middle stripe on the image) while others continue to lase. And the lowest energy stripe is generally on resonant in our recorded data. This feature is consistent with 3-D FEL simulations where we typically see multiple stripes based on the unlimited resolution of simulation results.

Tapering is a well-known method to achieving higher FEL power, and this diagnostic tool provides a direct measurement of the particle trapping which could help optimize the undulator taper setup.

Other Studies

With the capability to measure the electron bunch longitudinal phase space and to reconstruct X-ray power profile, the XTCAV enables many other studies at the LCLS for further understanding the machine and improving performance. For example, diagnostics for slotted foil mode [21] are very challenging. Using XTCAV, we see directly the emittance spoiling effects in the measured image [11, 13]. A recently developed two-bunch two-color mode also benefits greatly from this diagnostic tool when setting the machine configuration [22]. We also studied the microbunching instability at the LCLS and measured slice energy spread [13, 23], which is important for future machine design and seeding studies.

DISCUSSIONS

The XTCAV has been successfully installed and commissioned at the LCLS and now it serves an invaluable diagnostic that can operate at the full 120 Hz repetition rate of the machine. Since it is noninvasive to the operation, it provides an online tool for user experiments which is critical for experimental data alalysis. Furthermore, this also greatly helps machine physicists and operators understand and improve the machine performance.

The present measured resolution is about ~1 fs rms at soft X-ray energy, and ~4 fs rms at hard X-ray energy. To further improve the resolution, especially at the high energy side, a compact X-band SLED system is under design [24], which is expected to improve the resolution by a factor 2.

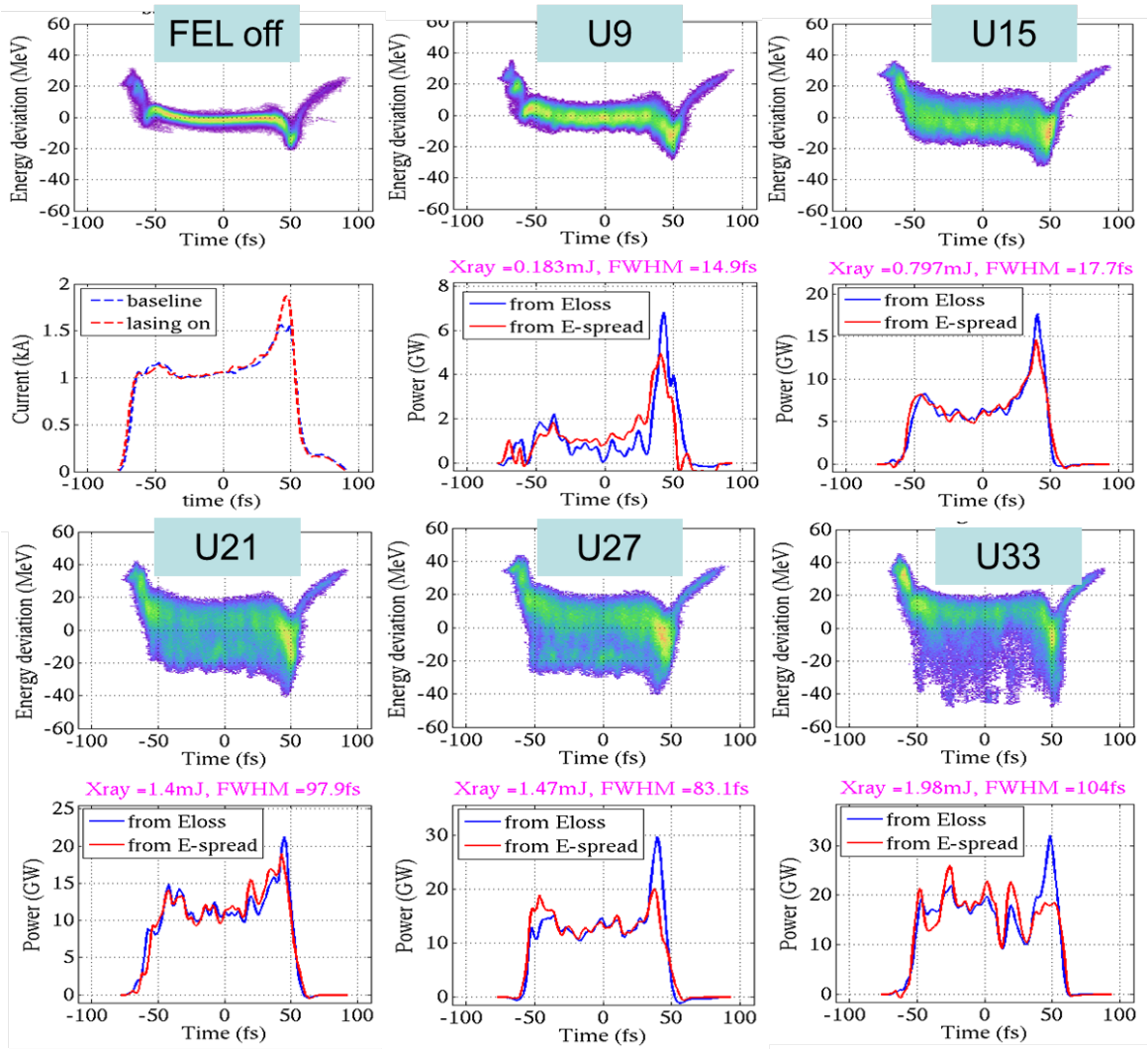

Figure 3: Temporal profile reconstruction. The electron bunch charge is 150 pC with an energy of 4.7 GeV to produce photons at 1.0 keV. The measured single-shot longitudinal phase space images are shown in (a): “lasing off" and (b): “lasing on". The reconstructed X-ray power profiles are shown in (c) from the time-dependent energy loss (blue curve) and energy spread growth (red curve). The bunch head is to the left in these plots and throughout.

ACKNOWLEDGMENT

We thank SLAC engineering, controls, operations, safety, and rf support groups for their help and dedicated support. This work was supported by Department of Energy Contract No. DE-AC02-76SF00515.

REFERENCES

[1] W. Ackermann *et al. Nature Photon.* **1**, 336-342 (2007).

[2] P. Emma *et al. Nature Photon.* **4**, 641-647 (2010).

[3] T. Ishikawa *et al. Nature Photon.* **6**, 540-544 (2012).

[4] E. Allaria *et al. Nature Photon.* **7**, 913-918 (2013).

[5] S. Düsterer, *Proc. of SPIE* vol. **8078**, 80780H-1 (2011).

[6] Y. Ding *et al. Phys. Rev. ST Accel. Beams* **14**, 120701 (2011).

[7] C. Behrens *et al. Nature Communications*, **5**, 3762 (2014).

[8] G. A. Loew & O. H. Altenmueller, Design and applications of R.F. deflecting structures at SLAC, SLAC-PUB-135 (1965).

[9] P. Emma, J. Frisch & P. Krejcik, A transverse rf deflecting structure for bunch length and phase space diagnostics. SLAC LCLS technical Report LCLS-TN-00-12 (2000).

[10] P. Krejcik *et al.* Engineering design of the new LCLS X-band transverse deflecting cavity. Proceedings of IBIC2013, Oxford, UK, p. 167-169 (2013);

[11] T. J. Maxwell *et al.* Femtosecond-scale x-ray FEL diagnostics with the LCLS X-band Transverse DeïňĆector. SPIE conference, San Diego, 2014.

[12] P. Emma, An X-band transverse rf deflector for the LCLS, SLAC LCLS Technical Note (October 18, 2006).

[13] P. Krejcik *et al.* Commissioning the new LCLS X-band transverse deflecting cavity with femtosecond resolution . Proceedings of IBIC2013, Oxford, UK, p. 308-311 (2013);

[14] Y. Ding *et al.* Commissioning of the X-band transverse deflector at the Linac Coherent Light Source. Proceedings of IPAC13, p. 2091-2093, Shanghai, China (2013)

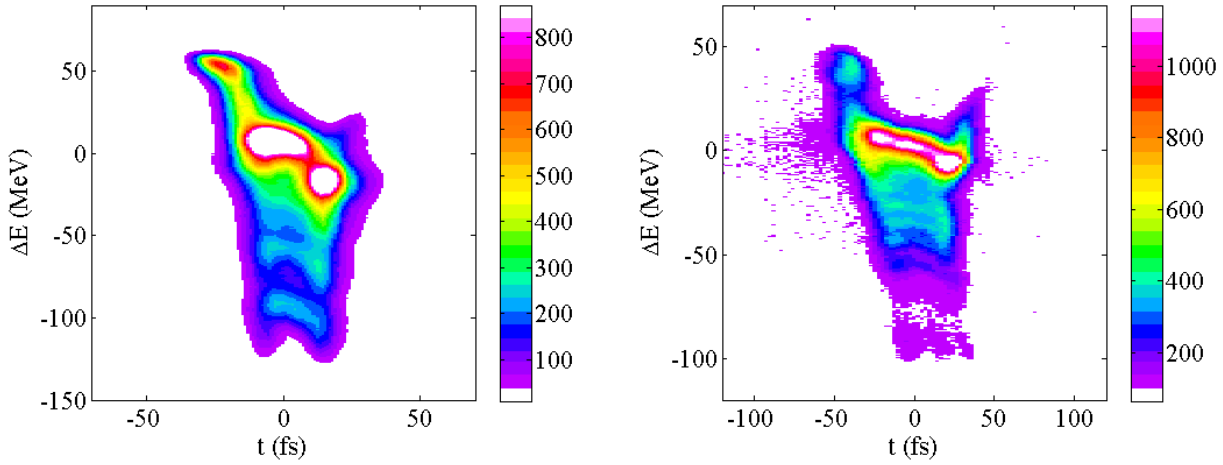

(a) 13.2 GeV (b) 11.6 GeV

Figure 4: Particle trapping. Measured electron beam longitudinal phase space images at electron energy 13.2 GeV and 11.6 GeV, at the end of the undulator. The isolated energy stripes from the trapping feature are clear at the low energy side of the phase space. We used a special color map from F. - J. Decker to enhance the visibility of the trapping [20].

[15] V. A. Dolgashev, Waveguide coupler for X-band defectors. SLAC-WP-084. Presented at 13th Advanced Accelerator Concepts Workshop, Santa Cruz, California, USA (2008).

[16] J. Wang & S. Tantawi, X-band traveling wave rf deflector structures. Proceedings of LINAC2008, 966-968, Tsukuba, Japan (2008).

[17] V. A. Dolgashev, & J. Wang, RF Design of X-band RF Deflector for Femtosecond Diagnostics of LCLS Electron Beam, *AIP Conf. Proc.* **1507**, 682 (2012).

[18] E. L. Saldin, E. A. Schnedmiller and M. V. Yurkov, The physics of free electron lasers, Springer;

[19] N. M. Kroll, P. L. Morton & M. N. Rosenbluth, *IEEE J. Quantum Electron.* **17**, 1436 (1981).

[20] F.-J. Decker, private communication.

[21] P. Emma *et al. Phys. Rev. Lett.* **92**, 074801 (2004).

[22] A. Marinelli et al, paper in preparation.

[23] D. Ratner et al., paper in preparation.

[24] Chen Xu, Juwen Wang and Sami Tantawi, THPP125, in this LINAC14 proceedings.